Piezoelectricity in Cellular Electret Films

J. Hillenbrand and G. M. Sessler
Institute for Communications Technology
Darmstadt University of Technology
Darmstadt, Germany

ABSTRACT

Permanently charged films with a cellular or porous structure represent a new family of polymer electrets. These materials show piezoelectric properties with high piezoelectric constants. The electromechanical response equations of such films are derived for their operation as sensors and as actuators. Experimental results are also presented for cellular polypropylene (PP). In particular, measurements of the direct and inverse piezoelectric constants in the frequency range 0 to 10 kHz and of the variation of these constants across the surface of the films are discussed. These measurements, performed by direct application of stress or by the use of a profilometer, an accelerometer and an interferometer yield a frequency-independent piezoelectric d_{33} constant of $\lesssim$ 220 pC/N. Assuming reasonable charge distributions and charge densities, the calculated piezoelectric constants are in good agreement with the measured values. The theoretical model shows the reciprocity of the piezoelectric constants.

1 INTRODUCTION

THERE has been considerable recent interest in the permanent charging of films with a cellular or porous structure [1–15]. It was shown that such films of polypropylene (PP), polytetrafluoroethylene, and silicon dioxide, when charged with corona or other methods, show relatively good electret behavior. These films can be used, either as single layers or together with another, less compliant layer, as reversible electromechanical or electroacoustic transducers. They exhibit piezoelectric properties and possess piezoelectric constants or sensitivities comparable to those of piezoelectric ceramics, but are mechanically better matched to air or water. This makes such materials attractive for a variety of applications [1].

In the present paper, the electromechanical response equations of such films are derived for their operation as piezoelectric sensors and as actuators, and the reciprocity of the transduction is shown. Following this, various experimental results are reported for cellular films of PP. These results demonstrate the piezoelectric activity of such films in the frequency range of 0 to 10 kHz in both directions and allow one to determine the piezoelectric constants. Finally, a comparison of the theoretical and experimental results yields information on the amount of charge and on its distribution in the cellular structure of the films.

2 RESPONSE EQUATIONS

2.1 MODEL OF CELLULAR FILM

Typical cross sections of a cellular film are shown in Figure 1. To allow for a ready analysis of the electromechanical operation of such films, a simplified structure (which cannot be used for a calculation of the elastic properties of the film), as shown in Figure 2 is considered. The charged material, electroded on top and bottom, consists of plane parallel solid layers and air layers of thicknesses s_{1n} and s_{2m}, respectively, with $n = 1, 2, \ldots N$ and $m = 1, 2, \ldots N-1$, where N is the total number of solid layers. It is further assumed that the two solid surfaces confining the m-th air layer carry a total planar charge density of σ_m and $-\sigma_m$, respectively, and that no volume charges exist. The quantity σ_m includes all permanent charges (surface charges and the ends of polarization chains, see [16], p. 13 ff.). The permanent charges on the two sides of each air gap are taken to be equal in magnitude since it is assumed that they originate from discharges in the air gap during poling (see Section 3.2.4). Figure 2 also shows the labelling of the electric fields E_{1n} and E_{2m} in the solid and air layers, respectively.

2.2 FIELD EQUATIONS

The electric fields in the solid layers and air layers may be obtained from the Gauss and Kirchhoff laws. For the uppermost solid-air interface, Gauss' law can be written as

$$-\varepsilon E_{11} + E_{21} = \frac{\sigma_1}{\varepsilon_o} \tag{1}$$

Similar relations hold for the other interfaces. Kirchhoff's second law is for short-circuit conditions

$$\sum_i s_{1i} E_{1i} + \sum_i s_{2i} E_{2i} = 0 \tag{2}$$

These equations yield $E_{11} = E_{12} = \cdots = E_1$ with

$$E_1 = -[\varepsilon_o(s_1 + \varepsilon s_2)]^{-1} \sum_j s_2 \sigma_j \tag{3}$$

and

$$E_{2i} = \frac{\sigma_1}{\varepsilon_o} - [\varepsilon_o(s_1 + \varepsilon s_2)]^{-1} \varepsilon \sum_j s_{2j} \sigma_j \tag{4}$$

1070–9878/0/ $3.00

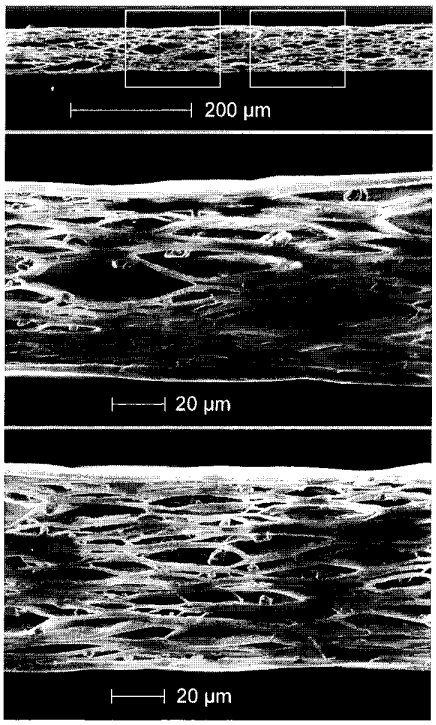

Figure 1. The scanning electron microscopy (SEM) images of the cross section of a larger (top) and two smaller (middle and bottom) segments of a 70 μm thick cellular PP film.

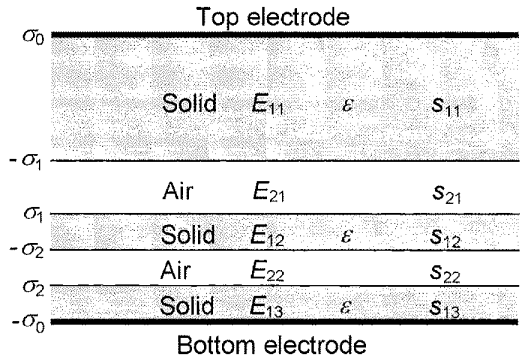

Figure 2. Simplified model of cellular film with $N = 3$.

where $s_1 = \sum_i s_{1i}$ and $s_2 = \sum_i s_{2i}$.

2.3 SENSOR RESPONSE FOR ELECTRICAL SHORT CIRCUIT

The charge on the top electrode is given by

$$\sigma_0 = -\varepsilon_o \varepsilon_1 E_1 \tag{5}$$

In short circuit, it depends on thickness changes of the film caused by an applied force. Since the thickness changes are primarily due to the compression of the air layers, the electrode charge is controlled by $\partial\sigma_0/\partial s_2$. If $\partial\sigma_{2i}/\partial s_2 = s_{2i}/s_2$ is assumed then $\partial\sigma_0/\partial s_2$ follows from Equations (3) and (5) as

$$\frac{\partial\sigma_0}{\partial s_2} = \varepsilon \frac{s_i \sum_i s_{2i}\sigma_i}{s_2(s_1 + \varepsilon s_2)^2} \tag{6}$$

In the quasi-static case (well below any resonance), a strain relation $\Delta s_2/s = \Delta p/Y$ holds, where s equals $s_1 + s_2$, Δp is the applied stress and Y is Young's modulus for the film. As shown in Section 3.2.2, Y is mainly determined by the stiffness of the polymer structure and to a lesser degree by the compressibility of the air in the voids. One obtains the piezoelectric constant $d_{33} = \Delta\sigma_0/\Delta p$ from Equation (6) in finite-difference form as

$$d_{33} = \frac{\Delta\sigma_0}{\Delta p} = \frac{\varepsilon s}{Y} \frac{s_i \sum_i s_{2i}\sigma_i}{s_2(s_1 + \varepsilon s_2)^2} \tag{7}$$

A similar equation was derived before for a two-layer system [17].

2.4 SENSOR RESPONSE FOR ELECTRICAL OPEN CIRCUIT

Under open-circuit conditions, the electrode charge σ_0 and thus the fields E_1 and E_{2i} remain constant. In particular, they do not change with sudden thickness changes of the air layers, but rather maintain their quiescent values which are assumed to be the short-circuit values. Thus, thickness changes induce a voltage

$$\Delta V = \sum_i \Delta s_{2i} E_{2i} \tag{8}$$

corresponding to a mean electric field

$$\Delta E = -\frac{1}{s} \sum_i \Delta s_{2i} E_{2i} \tag{9}$$

Using again the above strain relation and Equation (4), one obtains the open-circuit piezoelectric constant

$$g_{33} = \frac{\Delta E}{\Delta p} = \frac{1}{\varepsilon_o Y} \frac{s_i \sum_i s_{2i}\sigma_i}{s_2(s_1 + \varepsilon s_2)} \tag{10}$$

In this open-circuit mode of operation, the sensor reduces to a conventional capacitor microphone if one assumes just a single layer of dielectric and a single layer of air (thicknesses s_1 and s_2, respectively).

Thus Equation (10) yields below resonance

$$g_{33} = \frac{s_1 \sigma}{\varepsilon_o Y(s_1 + \varepsilon s_2)} \tag{11}$$

For capacitor microphones, sg_{33} is usually referred to as sensitivity. If the air gap controls the restoring force, s/Y is replaced by $s_0/\gamma p_0$, where s_0 is the thickness of the air cavity, γ is the ratio of the specific heats and p_0 is the air pressure ([16], p. 349).

2.5 ACTUATOR RESPONSE FOR MECHANICALLY FREE-RUNNING SYSTEM

An applied ac or dc voltage ΔV generates additional fields e_1 and e_2 in the solid and air layers, respectively, of the film such that

$$\Delta V = e_1 s_1 + e_2 s_2 \tag{12}$$

The field e_2 in the air gaps causes an additional force per unit area between any two dielectric layers given by

$$\Delta F_{2i} = \varepsilon_o e_2 E_{2i} \tag{13}$$

which, in turn, causes in a mechanically free-running system a thickness change of the air layer Δs_2i. The sum of these thickness changes is

$$\Delta s = \sum_i \Delta s_{2i} = \frac{s}{Y s_2} \sum_i s_{2i} \Delta F_{2i} \tag{14}$$

With Equation (4), (12), and (13), one obtains the inverse piezoelectric constant from Equation (14)

$$\frac{\Delta s}{\Delta V} = \frac{\varepsilon s}{Y} \frac{s_1 \sum_i s_{2i}\sigma_i}{s_2(s_1 + \varepsilon s_2)^2} \tag{15}$$

From this relation, the ratio $\Delta S/\Delta\sigma_0 0$, where ΔS is the mechanical strain $\Delta s/s$, may be obtained

$$\frac{\Delta s}{\Delta \sigma_0} = \frac{1}{\varepsilon_o Y} \frac{s_1 \sum_i s_{2i}\sigma_i}{s_2(s_1 + \varepsilon s_2)} \tag{16}$$

2.6 RECIPROCITY RELATIONS

The above equations obey, as expected, the reciprocity relations for reversible systems [18]. Using the four-pole equations in admittance form and applying the impedance analogy to one side of the four pole, the reciprocity relation can be written as

$$\frac{\Delta \sigma_0}{\Delta p} = \frac{\Delta s}{\Delta V} = d_{33} \tag{17}$$

which is also found from Equation (7) and (15). If the four-pole equations are expressed in impedance form and if the mobility analogy is used, the reciprocity relation reads

$$\frac{\Delta E}{\Delta p} = \frac{\Delta S}{\Delta \sigma_0} = g_{33} \tag{18}$$

which, in turn, follows from Equation (10) and (16). The expressions in Equation (17) and (18) correspond to the piezoelectric charge and voltage constants, respectively [19].

3 MEASUREMENTS

All measurements presented were performed with PP ?? (EMF) films [1, 20] (HS01, from VTT, Finland) of 70 μm thickness, covered on both sides with aluminum electrodes. The corona charging process was carried out by the manufacturer of the films. Measurements corresponding to the direct as well as the inverse longitudinal piezoelectric effect are presented in this Section.

3.1 MEASURING METHODS

3.1.1 DIRECT PIEZOELECTRIC CONSTANT

Mechanical stress was manually applied to and removed from the films on a time scale of $\sim$1 s. The charges generated were measured with a charge amplifier (Brüel & Kjaer 2635) and the output signal of the amplifier was recorded with a digital storage oscilloscope (Philips PM3350) and an ancillary PC. The ratio of generated charge density to applied pressure is the quasi-static direct piezoelectric d_{33} constant.

3.1.2 INVERSE PIEZOELECTRIC CONSTANT

In the frequency range from 10 to 30 Hz a profilometer (Veeco Instruments Dektak 8000) was used for these measurements. A sinusoidal voltage (V_{rms}<350 V) was applied to the EMF samples while the surface vibration was recorded by the profilometer. Profile scans with this instrument are made electromechanically by moving the film beneath a diamond-tipped stylus which rides over the surface of the sample. The relevant quantity, *i.e.* the amplitude of the periodic thickness change as function of the surface position, was obtained by applying a digital bandpass filter to the raw data. The ratio of thickness change to applied voltage yields the inverse piezoelectric d_{33} constant.

Measurements of the inverse d_{33} constant for frequencies from 10 Hz to 10 kHz were performed with an accelerometer (Brüel & Kjaer 4344), which was connected to a charge amplifier (Brüel & Kjaer 2635) whose output was fed into a lock-in amplifier (EG&G Instruments 5110). The EMF samples were excited with sinusoidal voltages (V_{rms}<100 V) and the displacements of the surfaces were calculated from the measured accelerations. The ratio of displacement to applied voltage yields the inverse piezoelectric d_{33} constant.

In the experimental setup, one side of a glass plate with an area of 2.5 cm^2 and 1 mm thickness was glued to the film surface and the accelerometer with a mass of 30 g was bonded to the other side. This enlargement of the contact area shifts the resonance frequency of the mass/spring system accelerometer/film to a higher frequency ($\sim$1.5 kHz) and allows measurements of the piezoelectric constant to 10 kHz. Reference measurements in the frequency range of 0 to 300 kHz were made also with two different Michelson interferometers. For these measurements, the samples were excited electrically with sinusoidal voltages and the vibration amplitudes were determined. The results of these measurements will only be discussed briefly for comparison purposes.

3.2 EXPERIMENTAL RESULTS

3.2.1 DIRECT PIEZOELECTRIC CONSTANT

An example of a measurement of the direct effect, performed as described in Section 3.1.1, is presented in Figure 3. The time of applying and removing the force of 3.8 N is marked in the figure. The slow variation of the charge during times of constant force is due to the charge amplifier. The analysis of Figure 3 yields a piezoelectric constant of 220 pC/N. Further measurements, performed with other HS01 films using different stress, yielded comparable mean piezoelectric constants.

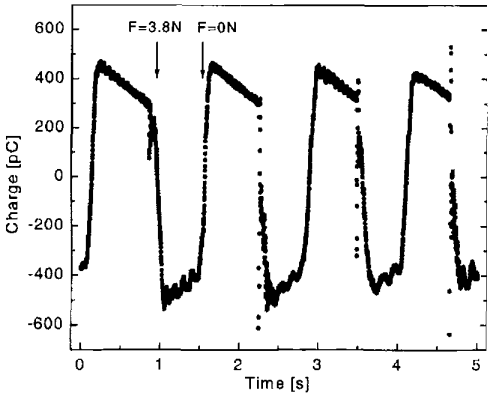

Figure 3. Change of output signal of the charge amplifier upon periodic application and removal of a force of 3.8 N to an EMF film.

3.2.2 INVERSE PIEZOELECTRIC CONSTANT

In Figure 4 measurements with the profilometer (see Section 3.1.2) of the inverse piezoelectric effect are presented. All measurements were

performed at exactly the same surface position of the film with a laterally fixed stylus. The film was excited with a frequency $f = 13.64$ Hz and at different voltages. Bandpass filtering at 13.64 and 27.27 Hz was performed and the mean vibration amplitudes were calculated. At 13.64 Hz a linear relation between these amplitudes and the applied voltages can be found, rendering an inverse piezoelectric constant of 176 pm/V = 176 pC/N.

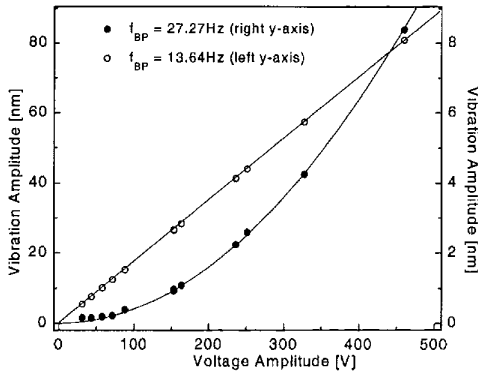

Figure 4. Mean amplitudes of the surface vibration after bandpass filtering at 13.64 and 27.27 Hz. The EMF film was excited with different voltages at 13.64 Hz.

For the second harmonic at 27.27 Hz, a quadratic dependence of the vibration amplitudes *vs.* the voltage was observed in our measurements (closed symbols in Figure 4). This electrostrictive effect is due to the electrostatic forces between the two electrodes and therefore should be independent of the electret charges. This independence was confirmed by measurements on thermally depolarized films.

For Young's modulus a value of $Y = 9.5{\times}10^5$ Pa for a film of 70 μm thickness was calculated from the data for 27.27 Hz in Figure 4. This value is mostly determined by the stiffness of the polymer structure since the contribution of the compressibility of the air in the voids amounts only to $Y' = o_0 s_2/s$, where p_0 is the air pressure. Thus, $Y' = 1.6{\times}10^5$ N/m^2, indicating that $Y' \ll Y$.

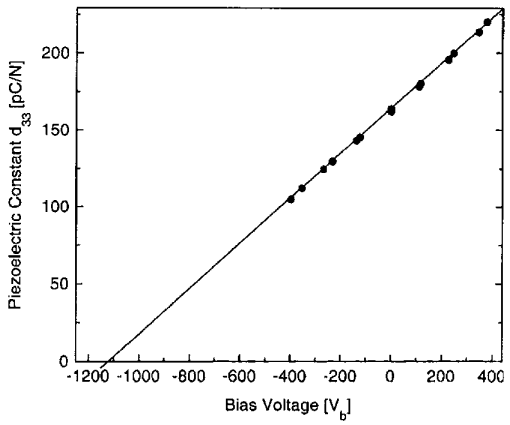

Figure 5. Piezoelectric d_{33} constant of an EMF film as function of applied bias voltage V_b.

The magnitude of the piezoelectric constant of an EMF film can be influenced by an additional dc-voltage (which is normally not present) applied to the electrodes since this external voltage alters the electric field inside the air voids. Figure 5 presents profilometer measurements of the variation of the inverse piezoelectric constant as function of the bias voltage V_b applied in addition to the sinusoidal voltage of $V_{\text{rms}} = 110$ V at 13.64 Hz. A linear dependence was found. Extrapolating the measured data to $d_{33} = 0$ yields a voltage of ~ -1100 V. This is obviously the voltage that cancels the field in the air voids.

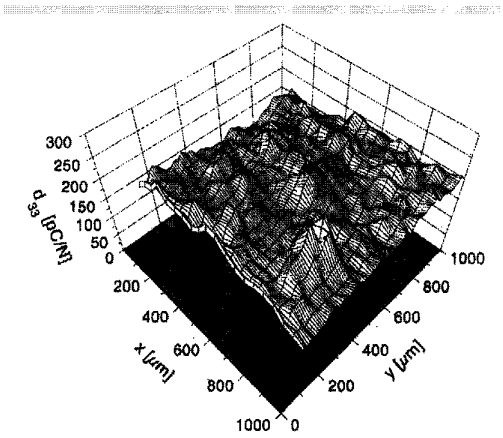

Figure 6. Inverse piezoelectric constant d_{33} of an EMF film measured within an area of 1× 1 mm^2.

To eliminate the influence of a locally varying piezoelectric constant, the preceding measurements were performed on a single point of the surface. In contrast, Figure 6 presents the variation of the piezoelectric constant d_{33} of an EMF film within an area of 1 mm^2. For this measurement 20 scans of 1000 μm length and 50 s duration were performed. A voltage of $V_{\text{rms}} = 280$ V at 27.27 Hz was applied to the EMF film during the measurement. The first and the last of these scans are shown again in Figure 7. The non-uniformity of d_{33} is expected to be due to the cellular structure, which has typical dimensions of 30 to 50 μm (see Figure 1).

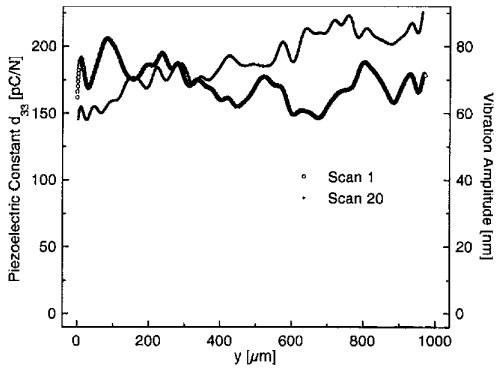

Figure 7. First and last scan of the piezoelectric profiles shown in Figure 6.

To clarify this question, the relationship between d_{33} and Young's modulus is presented in Figure 8. In this measurement the film was excited with a voltage of $V_{\text{rms}} = 280$ V at 13.64 Hz and a scan of 600 μm length was performed. It can be seen that the vibration amplitude of the fundamental (proportional to d_{33}) and the second harmonic (inversely

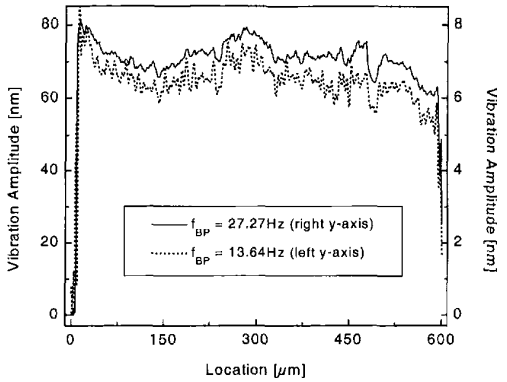

Figure 8. Vibration amplitudes of the fundamental and second harmonic of an EMF film, excited with a voltage of $V_{rms} = 280$ V at 13.64 Hz.

proportional to Young's modulus) are approximately proportional. This indicates that the variations in d_{33}, as seen in Figures 6 and 7, are to a large degree caused by lateral fluctuations in Young's modulus. These are, of course, due to the cellular structure with the typical dimensions of about 50 μm mentioned above.

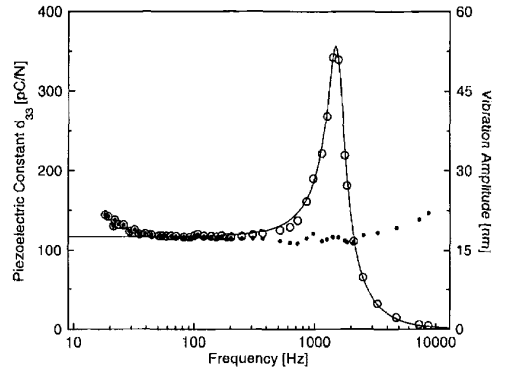

Figure 9. Measured vibration amplitude of an EMF film (open circles) and best-fit curve (solid line) calculated for a damped mass/spring resonance. Also shown is the piezoelectric d_{33} constant (full circles) calculated from the vibration amplitude data with resonance analytically eliminated (see text).

The profilometer used in the measurements is restricted to frequencies below 30 Hz. To extend the frequency range of the piezoelectric measurements, the thickness vibration amplitudes of the EMF films were determined indirectly by measuring the acceleration of the film surface, as described in Section 3.1.2. From the measured acceleration the displacements (vibration amplitudes) were calculated. They are shown in Figure 9 together with the corresponding inverse piezoelectric constants. These measurements indicate an almost frequency independent d_{33} constant of $\sim$ 120 pC/N between 20 and 500 Hz. The slight increase toward lower frequencies could not be confirmed with measurements (not shown) with a commercial Michelson interferometer which yielded constant d_{33} values between 0 and 500 Hz.

At higher frequencies, the above-mentioned resonance due to the film stiffness (Young's modulus) and the mass of the accelerometer determines the behavior of the displacement data in Figure 9. After peaking at the resonance frequency of 1.5 kHz, the displacement drops off proportional to $1/\omega^2$ at higher frequencies. A best-fit resonance curve, calculated on the basis of a damped mass/spring system, is also shown in Figure 9. Since the resonance is external to the film, its effect on the piezoelectric constant should be eliminated. This was achieved by using displacements obtained by dividing the measured displacements by the values of the best-fit curve.

The resulting d_{33}-values shown in Figure 9 are fairly frequency independent up to $\sim$5 kHz. This is also evident from measurements with a second Michelson interferometer [21]. These measurements demonstrate the frequency independence of the piezoelectric constants in the frequency range from 300 Hz to 200 kHz.

The results for d_{33} determined with the profilometer at 13.64 and 27.27 Hz ($\sim$ 176 and 150 pC/N, see Figures 4 and 6, respectively) agree fairly with the data in Figure 9. The differences between these measurements can be explained by the fact that the d_{33} constant is not only subject to small-scale variations (see Figures 6 and 7) but differs even more considerably on a larger scale, such as between different samples. Also, systematic measuring errors may contribute to the difference of results obtained by the various experimental methods. The significantly higher quasi-static d_{33} constant (220 pC/N, see Section 3.2.1) may be due to the much larger displacement (typically 1 μm as opposed to $\approx$10 nm for the other measurements) if one assumes that Young's modulus is displacement dependent. Also to be considered is the fact that the quasi-static method measures the direct piezoelectric effect while all the other methods measure the inverse piezoelectric effect. There may be some physical reason that the direct and inverse piezoelectric constants differ due to the electrical and mechanical inhomogeneities of the film.

3.2.3 THERMAL STABILITY

Another series of measurements was taken to investigate the thermal stability of the piezoelectric constants. The films were heated at a constant temperature (60 or 80°C) for a time period of $\sim$ 30 min. Then, the film was cooled down to room temperature and its piezoelectric constant was measured. Several such annealing and measuring cycles were applied to the samples. As shown elsewhere [5], the piezoelectric constant decreased to approximately half of its original value in five hours at 80°C.

3.2.4 CHARGE DISTRIBUTION

In order to obtain information about the polarity of the surface charges within an EMF film, a voltage step not causing any discharge in the film was applied, and the direction of the resulting thickness change was measured. Positive voltage steps applied to an already positively charged film increased the thickness of the film. This result can be explained if discharges occur in the air gaps during poling. This mechanism has been assumed to be responsible for the charging in previous studies.

4 DISCUSSION AND CONCLUSIONS

For a comparison of the experimental results with theory, an evaluation of Equation (7) and (15) is necessary. From the constants in these equations, $\varepsilon = 2.35$, $Y = 9.5\times10^5$ Pa (for 27.27 Hz, see Section 3.2.2),

$s = 70$ μm, $s_1 = 26$ μm, $s_2 = 44$ μm (s_1 and s_2 are determined from the densities) are known. The remaining quantities s_{2i} and σ_i have to be estimated. From microphotographs such as Figure 1 it can be inferred that there are $\sim$ 10 voids of >2 μm thickness and a larger number of smaller voids across a 70 μm thick film. Assuming further that only the surfaces of the large voids are charged and that $\sigma_i = 10^{-3}$ C/m^2, one obtains $d_{33} \approx 200$ pC/N (or pm/V) in agreement with the above data at low frequencies and [1, 8, 9]. The assumed charge density yields from Equation (4) a voltage of <150 V even across large voids, which is below the Paschen voltage of $\approx$400 V for such gaps. This indicates that the above model for the piezoelectric behavior of the cellular material is based on reasonable assumptions.

Cellular films also can be used for microphones or hydrophones. From Equation (10), sensitivities of $\sim$ 1.7 mV/Pa, corresponding to -55 dB *vs.* 1 V/Pa, are expected below resonance. Actually, a microphone sensitivity of $\sim$ 2 mV/Pa was found in another study [22]. This value and relatively high sensitivity show that cellular electrets also are useful in such applications.

ACKNOWLEDGMENT

The authors are grateful to Profs. Siegfried Bauer (Linz) and Reimund Gerhard-Multhaupt (Potsdam) for stimulating discussions. They are further indebted to VTT Chemical Technology for providing the EMF material and to the Deutsche Forschungsgemeinschaft (DFG) for financial support.

REFERENCES

[1] J. Lekkala, R. Poramo, K. Nyholm and T. Kaikkonen, "EMF force sensor - a flexible and sensitive electret film for physiological applications", Med. & Bio. Eng. & Comp., Vol. 34, Suppl. 1, Pt. 1, pp. 67–68, 1996.

[2] Z. Xia, J. Jian, Y. Zhang, Y. Cao and Z. Wang, "Electret Properties for Porous Polytetrafluoroethylene (PTFE) Film", 1997 Annual Report, Conference on Electrical Insulation and Dielectric Phenomena, pp. 471–474, 1997.

[3] Y. Cao, Z. Xia, Q. Li, L. Chen and B. Zhou, "Electret properties of silicon dioxide aerogels", Proc. 9th International Symposium on Electrets, pp. 40–45, 1996.

[4] Z. Xia, A. Wedel and R. Danz, "The Excellent Charge Storage Stability of Porous Polytetrafluoroethylene (PTFE) Film Electrets", Proc. 10th International Symposium on Electrets, 1999, pp. 23–26.

[5] G. M. Sessler and J. Hillenbrand, "Electromechanical Response of Cellular Electret Films", Proc. 10th International Symposium on Electrets, pp. 261–264, 1999.

[6] R. Gerhard-Multhaupt, Z. Xia, W. Künstler and A. Pucher, "Preliminary study of multi-layer space-charge electrets with piezoelectric properties from porous and non-porous Teflon films", Proc. 10th International Symposium on Electrets, pp. 273–276, 1999.

[7] R. Schwödiauer, G. Neugschwandtner, S. Bauer-Gogonea, S. Bauer, J. Heitz and D. B uerle, "Dielectric and electret properties of novel Teflon PTFE and PTFE-like polymers", Proc. 10th International Symposium on Electrets, pp. 313–316, 1999.

[8] M. Paajanen, H. Välimäki and J. Lekkala, "Modeling the sensor and actuator operations of the ElectroMechanical Film EMFi", Proc. 10th International Symposium on Electrets, pp. 735–738, 1999.

[9] J. Lekkala and M. Paajanen, "EMFi - New Electret Material for Sensors and Actuators", Proc. 10th International Symposium on Electrets, pp. 743–746, 1999.

[10] J. van Turnhout, R. E. Staal, M. Wübbenhorst and P. H. de Haan, "Distribution and Stability of Charges in Porous Polypropylene Films", Proc. 10th International Symposium on Electrets, pp. 785–788, 1999.

[11] J. Hillenbrand and G. M. Sessler, "Mechanical and Electrical Response of Charged Polymers with Cellular Structure", 1999 Annual Report, Conference on Electrical Insulation and Dielectric Phenomena, pp. 43–46, 1999.

[12] Z. Xia, R. Gerhard-Multhaupt, W. Künstler, A. Wedel and R. Danz, "High surface-charge stability of porous polytetrafluoroethylene electret films at room and elevated temperatures", J. Phys. D: Appl. Phys., Vol. 32, pp. L83–L85, 1999.

[13] G. M. Sessler and J. Hillenbrand, "Electromechanical Response of Cellular Electret Films", Appl. Phys. Lett., Vol. 75, pp. 3405–3407, 1999.

[14] W. Künstler, Z. Xia, T. Weinhold, A. Pucher and R. Gerhard-Multhaupt, "Piezoelectricity of porous polytetrafluoroethylene single- and multiple-film electrets containing high charge densities of both polarities", Appl. Phys. A, Vol. 70, pp. 5–8, 2000.

[15] G. S. Neugschwandtner, R. Schwödiauer, S. Bauer-Gogonea and S. Bauer, "Large piezoelectric effects in charged, heterogeneous fluoropolymer electrets", Appl. Phys. A, Vol. 70, pp. 1–4, 2000.

[16] G. M. Sessler (ed.), *Electrets*, Vol. 1 (3rd Edition), Laplacian Press, 1999.

[17] R. Kacprzyk, A. Dobrucki and J. B. Gajewski, "Double-layer electret transducer", J. Electrostat., Vol. 39, pp. 33–40, 1997.

[18] P. M. Chirlian, *Basic Network Theory*, McGraw Hill, New York, 1969.

[19] D. A. Berlincourt, D. Curran and H. Jaffe, "Piezoelectric and Piezomagnetic Materials and their Function in Transducers", in: W. P. Mason, *Physical Acoustics* Vol. I, Part A, Academic Press, New York, pp. 169–270, 1964.

[20] A. Savolainen and K. Kirjavainen, "Electrothermomechanical Film. Part I. Design and Characteristics", J. Macromol. Sci. A, Vol. 26, pp. 583–591, 1989.

[21] M. Vieytes, R. Schwödiauer, G. S. Neugschwandtner, S. Bauer-Gogonea, S. Bauer, J. Hillenbrand, R. Kressmann, G. M. Sessler, M. Paajanen and J. Lekkala, "Nonpolar polymer foams: From symmetry breaking by charging to strong dynamic piezoelectricity", to be published.

[22] R. Kreßmann, M. Fischer and H. Berger, "Akustische Sensoren und Aktoren aus aufgeladenem, porösem Polypropylen", in: VDI Berichte Nr. 1530, Sensoren und Meßsysteme 2000, VDI Verlag, Düsseldorf, pp. 735–743, 2000.

This manuscript is based on a paper given at the 10th International Symposium on Electrets, Delphi, Greece, 22–24 September 1999.

Manuscript was received on 17 March 2000, in revised form 5 May 2000.